

Sequence-to-Sequence Neural Diarization with Automatic Speaker Detection and Representation

Ming Cheng, Yuke Lin, Ming Li* Senior Member, IEEE

Abstract—This paper proposes a novel Sequence-to-Sequence Neural Diarization (SSND) framework to perform online and offline speaker diarization. It is developed from the sequence-to-sequence architecture of our previous target-speaker voice activity detection system and then evolves into a new diarization paradigm by addressing two critical problems. 1) **Speaker Detection:** The proposed approach can utilize incompletely given speaker embeddings to discover the unknown speaker and predict the target voice activities in the audio signal. It does not require a prior diarization system for speaker enrollment in advance. 2) **Speaker Representation:** The proposed approach can adopt the predicted voice activities as reference information to extract speaker embeddings from the audio signal simultaneously. The representation space of speaker embedding is jointly learned within the whole diarization network without using an extra speaker embedding model.

During inference, the SSND framework can process long audio recordings blockwise. The detection module utilizes the previously obtained speaker-embedding buffer to predict both enrolled and unknown speakers' voice activities for each coming audio block. Next, the speaker-embedding buffer is updated according to the predictions of the representation module. Assuming that up to one new speaker may appear in a small block shift, our model iteratively predicts the results of each block and extracts target embeddings for the subsequent blocks until the signal ends. Finally, the last speaker-embedding buffer can re-score the entire audio, achieving highly accurate diarization performance as an offline system. Experimental results show that our proposed SSND framework achieves new state-of-the-art diarization error rates (DERs) for online inference on the DIHARD-II (24.41%) and DIHARD-III (17.12%) evaluation sets without using oracle voice activity detection. At the same time, it also refreshes the state-of-the-art performance for offline inference on these benchmarks, with DERs of 21.95% and 15.13%, respectively.

Index Terms—Speaker Diarization, Online Speaker Diarization, SSND

I. INTRODUCTION

SPEAKER diarization aims to split the conversational audio signal into segments with labeled identities, solving the problem of "Who-Spoke-When [1]." It is the core front-end speech processing technique in various downstream tasks like multi-speaker speech recognition, etc [2].

Early speaker diarization studies have widely investigated the cascaded methods that process audio signals through a series of independent modules [3]–[6]. Later, End-to-End Neural Diarization (EEND) methods [7]–[10] are proposed to estimate multiple speakers' voice activities as multi-label

classification, where the end-to-end model architecture can be directly optimized by the permutation-invariant training (PIT) [11]. Also, Target-Speaker Voice Activity Detection (TSVAD) approaches [6], [12], [13] combine the advantages of cascaded methods and end-to-end neural networks. A typical TSVAD-based system requires a prior diarization system (e.g., the cascaded method) to extract each speaker's acoustic footprint as the speaker enrollment. Then, a neural network-based module predicts all speakers' corresponding voice activities. This two-stage framework demonstrates highly accurate performance in popular benchmarks such as DIHARD-III [14] and VoxSRC21-23 [15]–[18].

However, the diarization systems mentioned above are natively designed to process pre-recorded audio offline, which means they cannot satisfy scenarios with low latency demand (e.g., real-time meeting transcription) [1]. For online speaker diarization, cascaded methods must modify all the built-in components to be capable of online inference, especially the inherent clustering algorithms [19], [20]. Online EEND systems can be implemented by only replacing the network architecture [21], [22] or using a buffer to trace the previous input-output pairs [23]–[25]. However, the speaker permutation problem is prone to be affected by the increasing number of speakers in long-form audios, which remains a challenge that has yet to be fully addressed. As the post-processing approach, TSVAD models natively process the audio signals blockwise except for acquiring pre-extracted speaker embeddings from the initial stage. Therefore, online TSVAD methods [26], [27] are proposed to enable self-generated speaker embeddings during blockwise inference. However, they must be integrated with another online VAD system to help detect the presence of new speakers. The practical use of these existing methods is difficult.

This paper proposes a novel speaker diarization framework compatible with online and offline inference, namely the Sequence-to-Sequence Neural Diarization (SSND). The SSND framework is built upon the sequence-to-sequence architecture of our previous work [13]. Differently, it can adopt partially enrolled speaker embeddings to output complete voice activities and then extract the missed target embedding simultaneously. In this way, the SSND framework is able to predict target-speaker voice activities of each coming audio block in real-time operation and progressively gather target embeddings for the subsequent blocks. After the first-pass diarization, the collected target embeddings can also be used to re-decode the entire audio as an offline system. The SSND framework has become fundamentally different from previous diarization systems, as it does not need both unsupervised

Ming Cheng, Yuke Lin and Ming Li are with the School of Computer Science, Wuhan University, Wuhan 430072, China, and also with Suzhou Municipal Key Laboratory of Multimodal Intelligent Systems, Data Science Research Center, Duke Kunshan University, Kunshan 215316, China.

* Corresponding author. E-mail: ming.li369@dukekunshan.edu.cn

clustering and permutation-invariant training at the same time. Therefore, we name it as a new neural diarization approach. The contributions are summarized as follows.

- 1) We propose a novel masked speaker prediction method. One of the input speaker embeddings may be randomly erased during training. Then, the model learns to associate the output of the masked speaker with a learnable pseudo-speaker embedding, solving the one-to-one mapping problem between input speaker embeddings and output voice activities.
- 2) We propose a novel target-voice speaker embedding extraction method. In contrast to the previous TSVAD method, it utilizes the predicted voice activities as reference information to extract target embeddings from the input audio further. The embedding space of speaker detection and representation is jointly learned.
- 3) A simple but effective knowledge distillation strategy is developed to explore the potential of our proposed method when meeting large-scale data. We evaluate our approach on several widely-used datasets, outperforming previous state-of-the-art results in various online and offline evaluation settings.
- 4) The designed framework combines characteristics of both EEND and TSVAD methods. It is clustering-free and PIT-free, but can utilize the end-to-end neural network to discover possible unknown speakers. Meanwhile, the use of target embeddings maintains recognized speaker identities consistent across different blocks in long audio, which is usually the advantage of TSVAD-based methods.

II. RELATED WORKS

A. Offline Diarization

The cascaded speaker diarization consists of several components. 1) Voice Activity Detection (VAD) [28] removes non-speech regions from the audio. 2) Speech regions are divided into shorter segments [29], [30]. 3) Speaker embeddings (e.g., i-vectors [31], x-vectors [32]) are extracted from the speech segments and clustered into different identities by K-Means [3], AHC [30], SC [4], or others. 4) Post-processing techniques for overlapped speech regions can be optionally implemented [33], [34]. The number of output speakers is determined by the clustering algorithms.

End-to-End Neural Diarization (EEND) [7], [8] predicts multiple speakers' voice activities by formulating the diarization problem as a multi-label classification task. The original EEND models have a fixed number of output speakers restricted by their network architecture. Although using Encoder-Decoder based Attractor (EDA) [9], [10] can infer the variable number of speakers. In practice, the number of output speakers is still capped by the training data [35]. To solve this problem, integrating the end-to-end and clustering approach is a promising direction. For example, EEND-vector clustering (EEND-VC) [36]–[38] deploys an EEND model for shortly divided audio blocks and addresses the inter-block speaker permutation ambiguity by clustering of speaker embeddings. EEND-GLA [25], [39] computes local attractors for each

short block and determines speaker correspondence based on similarities between inter-block attractors. Also, several extensions of EEND are proposed from the aspects of network architecture [40]–[42], objective function design [43], [44], self/semi-supervised learning [45], [46], and so on.

Target-Speaker Voice Activity Detection (TSVAD) [12] is also effective. It relies on a prior diarization system to extract each speaker's acoustic footprint (i-vector) as enrollment. Then, the TSVAD model uses speech features (e.g., MFCC) and extracted i-vectors to output target speaker voice activities according to the enrollment order. Later, He et al. [47] adapt the model to handle a variable number of speakers by setting a maximum speaker limit and producing null voice activities for zero-padded ones. Sequential models (e.g., LSTM [48] and Transformer [49]) are implemented on the speaker dimension of model input to manage a variable number of speakers. To explore more discriminative speaker embeddings as an alternative to i-vector, Wang et al. [6] replace the front-end of the TSVAD model with a pre-trained extractor tailored for frame-level x-vectors. This modification demonstrates superior performance than a simple swap of i-vectors for x-vectors in early attempt [12]. Furthermore, the TSVAD framework has been investigated in various aspects (e.g., multi-channel signal [50], multi-modal system [51]–[53], joint inference with ASR [54], generative approach [55]).

B. Online Diarization

In an online scenario, the diarization system must make continual decisions on each audio frame while the conversation continues. This paradigm is crucial for low-latency applications such as real-time conversation transcription.

To extend cascaded methods to online inference, all built-in modules (e.g., voice activity detection, speech segmentation, speaker embedding extraction) must be executed in real time. Several techniques (e.g., UIS-RNN [56], UIS-RNN-SML [57]) replace the speech segmentation and speaker clustering with supervised neural networks. As the most critical component, online speaker clustering attracts much research interest, e.g., modified clustering [19], [58], PLDA-scoring [59], and clustering guided embedding extractor training [60]. However, their time complexity will increase with the number of speech segments, resulting in inadequate performance for long audio.

The extension of end-to-end approaches to online diarization can be broadly divided into two directions. The first is to train models that can convey information during block-wise or frame-wise inference to address the speaker permutation ambiguity. For instance, BW-EDA-EEND [21] adopts Transformer-XL [61] with recursive hidden states to take block-wise inputs, where the hidden states obtained from the previous blocks are used to generate attractors of the current block. Liang et al. [22] propose the frame-wise EEND (FS-EEND) to adaptively update speaker attractors frame by frame, which has a lower inference latency. In this direction, online diarization models can be easily optimized in a fully end-to-end manner. However, independent network architectures are required rather than offline diarization models. If both offline and online diarization models are needed, the deployment

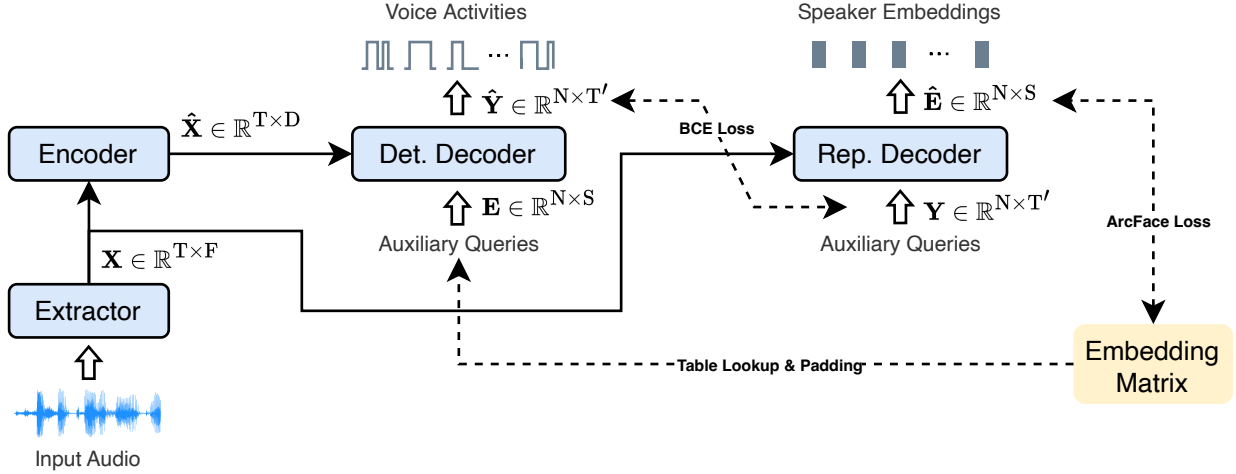


Fig. 1. The Sequence-to-Sequence Neural Diarization (SSND) framework. *Det.* and *Rep.* denote the abbreviations of detection and representation, respectively.

costs will be doubled. The second direction is to modify offline models for online inference. Speaker-tracing buffer (STB) [23], [24] is proposed to maintain the preceding results of EEND models during online inference. It makes the order of output speakers consistent without changing the network architecture. On top of this direction, EEND-GLA [25], [39] further integrates local and global attractors with STB for online inference, achieving state-of-the-art performance on multiple datasets. It is reported that STB can minimize the inference latency using a small block size and outperform BW-EDA-EEND [24], [25]. Nonetheless, this approach demands extra computations because every past frame in the buffer must be re-computed for each new block.

On the success of offline TSVAD methods [14]–[17], diverting the TSVAD framework for online inference is also a promising direction. In offline scenarios, TSVAD methods usually serve as post-processing to refine cascaded diarization results [12]. After obtaining target-speaker embedding from the initial stage, TSVAD models process audio signals block-wise. This property implies that TSVAD models can be naturally adapted to online inference if target-speaker embeddings are acquired in real time. Therefore, Wang et al. [26] firstly present the online TSVAD framework and then adapt it to multi-channel data [27]. Chen et al. [62] design a dictionary learning module across different frequency bands in multi-channel data to reduce the inference cost. Nevertheless, two critical problems prevent existing online TSVAD methods from practical use. 1) They rely on an additional VAD module to remove silent audio segments and detect the presence of unenrolled speakers during inference. The VAD errors might severely impact the final system output. 2) They utilize local speaker labels within each recording to optimize target embedding extraction, where the power of global speaker modeling is not fully exploited. In contrast, current advanced speaker verification techniques are mainly based on unique speaker identities over the whole training set [63].

Notably, the concepts of TSVAD and EEND families are becoming closer. In early TSVAD systems [6], [12],

[13], speaker embeddings are typically acoustic footprints extracted by speaker verification models (e.g., i-vectors [31], x-vectors [32]). Then, works of [26], [27] turn to generate speaker embeddings within TSVAD models. On the other hand, the attractors used in EEND systems [9], [10] are also a kind of local speaker embeddings within each audio block. Recent studies of [22], [25] begin to constrain the speaker similarity of attractors across different audio blocks. Obvious, using a set of embedding vectors to represent speaker identities has been widely adopted with different terminologies. Therefore, in this work, we aim to take advantage of both EEND and TSVAD methods to newly propose the SSND framework, achieving state-of-the-art performance on various multi-scenario datasets.

III. SEQUENCE-TO-SEQUENCE NEURAL DIARIZATION

A. Architecture

The proposed SSND framework takes the sequence-to-sequence architecture used in our previous offline method [13] with a few modifications, shown in Fig. 1.

1) *Extractor*: The ResNet-based [64] model is adopted as the front-end extractor. The audio signal is firstly transformed into log Mel-filterbank energies. Then, it is fed into the extractor with segmental statistical pooling (SSP) [6] to obtain frame-level speaker embeddings $\mathbf{X} \in \mathbb{R}^{T \times F}$, where T and F denote the length and dimension of extracted feature sequence. An additional linear layer can be employed to align the output dimension F with the input dimension of subsequent encoder and decoder modules, omitted to plot for clarity. This process converts raw audio signals into a sequence of neural network-based features.

2) *Encoder*: The Conformer-based [65] model is employed as the encoder to process the frame-level speaker embeddings. The input feature sequence is firstly added with sinusoidal positional encodings [66] and then fed into the encoder to obtain output feature sequence $\hat{\mathbf{X}} \in \mathbb{R}^{T \times D}$, where D is the attention dimension used in the encoder. This process further

takes long-term dependencies between frame-level speaker embeddings for the diarization task.

3) *Decoder*: The detection and representation decoders are based on the same network structure, shown in Fig. 2. Each decoder is made of several basic blocks. The input decoder embeddings of the first block are initialized by zeros and then processed by the following blocks. After the last output block, a simple linear transformation can be adopted to obtain the final predictions with desirable output shape. In detail, the proposed decoder block retains the main layout of the Speaker-wise Decoder (SW-D) [13] with a few changes.

- The cross-attention layer is placed before the self-attention layer. As the input embeddings of the first decoder block are initialized as zeros, there is no useful information for the self-attention layer at first.
- We define $F_q(\cdot)$ and $F_k(\cdot)$ to denote the fusion operations for input queries and keys, respectively. Let N denote the number of speakers. $\mathbf{X}_{\text{dec}} \in \mathbb{R}^{N \times D}$ and $\mathbf{Q}_{\text{aux}} \in \mathbb{R}^{N \times D'}$ represent the decoder embeddings and auxiliary queries, respectively. The $F_q(\cdot)$ operation is described as:

$$\mathbf{Q} = \mathbf{X}_{\text{dec}} + \text{Linear}_{\mathbb{R}^{D'} \rightarrow \mathbb{R}^D}(\mathbf{Q}_{\text{aux}})/\sqrt{D}, \quad (1)$$

where the linear transformation is deployed to align the dimension of queries and keys with the weight factor $1/\sqrt{D}$. Similarly, let $\mathbf{X}_{\text{fea}} \in \mathbb{R}^{T \times D}$ and $\mathbf{K}_{\text{pos}} \in \mathbb{R}^{T \times D'}$ represent the feature embeddings and positional embeddings with the length of T . The $F_k(\cdot)$ operation is described as:

$$\mathbf{K} = \mathbf{X}_{\text{fea}} + \text{Linear}_{\mathbb{R}^{D'} \rightarrow \mathbb{R}^D}(\mathbf{K}_{\text{pos}})/\sqrt{D}. \quad (2)$$

The fused queries \mathbf{Q} and keys \mathbf{K} are fed into the cross-attention layer with a Pre-LayerNorm method. Compared with the previous concatenation fusion, this additive fusion is more straightforward without expanding the output dimension of queries and keys.

- The auxiliary queries are L_2 -normalized in the detection decoder to guarantee that the input speaker embeddings lie in a hypersphere.

The difference between diarization and representation decoders is the input and output data. Let $\mathbf{E} \in \mathbb{R}^{N \times S}$ denote the given speaker embeddings with the number of N and the dimension of S . The ground truth of their target voice activities is denoted as a binary matrix $\mathbf{Y} \in \{0, 1\}^{N \times T'}$, where $y_{n,t'}$ represents the speaking existence of the n -th speaker at time t' . The detection decoder utilizes encoder output $\hat{\mathbf{X}}$ as feature embeddings and speaker embeddings \mathbf{E} as auxiliary queries to obtain the predicted voice activities $\hat{\mathbf{Y}} \in \{0, 1\}^{N \times T'}$. In contrast, the representation decoder utilizes extractor output \mathbf{X} as feature embeddings and voice activities \mathbf{Y} as auxiliary queries to obtain the predicted speaker embeddings $\hat{\mathbf{E}} \in \mathbb{R}^{N \times S}$. Two decoders perform inverse tasks to predict target-speaker voice activities and extract speaker embeddings simultaneously.

B. Training Process

The ground truth of \mathbf{Y} can be obtained from the adopted dataset during training. However, \mathbf{E} is not directly available

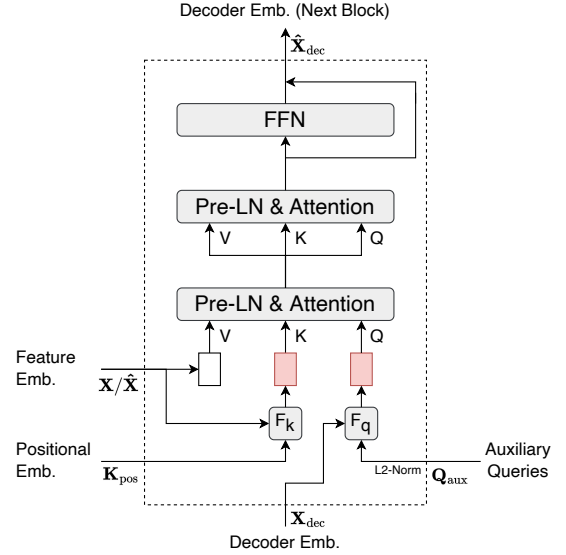


Fig. 2. The structure of the modified Speaker-wise Decoder. For clarity, the residual connections between attention layers are omitted from the plot.

because the embedding space must be learned by neural networks. To overcome this problem, we initialize a learnable embedding matrix $\mathbf{E}_{\text{all}} \in \mathbb{R}^{N_{\text{all}} \times S}$ to store the embedding vectors of all speakers in the training data, with the number of N_{all} and the dimension of S . All speaker labels are tokenized to N_{all} -dim one-hot vectors. For instance, the n -th speaker label can be denoted by the one-hot vector with zeros everywhere except its n -th value will be 1. Thus, given an input audio block with N_{loc} speaker labels $\mathbf{S}_{\text{loc}} \in \mathbb{R}^{N_{\text{loc}} \times N_{\text{all}}}$, the input speaker embeddings for the detection decoder can be obtained by $(\mathbf{S}_{\text{loc}} \times \mathbf{E}_{\text{all}}) \in \mathbb{R}^{N_{\text{loc}} \times S}$, which is a simple table look-up operation using matrix multiplication. After solving the input and output data, we propose two training approaches.

1) *Masked speaker prediction*: The masked language modeling (MLM) technique has been validated in natural language processing [67], conducted by randomly masking some words in the input text and then training the model to predict the masked words. Similarly, we introduce a masked speaker prediction method into speaker diarization. During training, one of the input speaker embeddings for each audio block will be randomly masked. The model learns to identify whether there is a person speaking in the audio block but without the given speaker embedding. In implementation, two padding strategies are proposed.

A learnable pseudo-speaker embedding $\mathbf{e}_{\text{pse}} \in \mathbb{R}^S$ is padded into the input speaker embeddings \mathbf{E} . For each training data, a probability is 0.5 that one existing speaker label $s_m \in \mathbf{S}$ will be randomly selected as the masked one. Accordingly, the speaker embedding \mathbf{e}_m will be removed from \mathbf{E} and the ground-truth of target voice activities $\mathbf{y}_m \in \mathbf{Y}$ will be re-assigned to the output of pseudo-speaker embedding. In this way, the model is trained to utilize the pseudo-speaker embedding to capture any unenrolled speaker's voice activities.

A learnable non-speech embedding \mathbf{e}_{non} is initialized. By setting the maximum speaker capacity of the model input to N , the missing input speaker embeddings less than N will

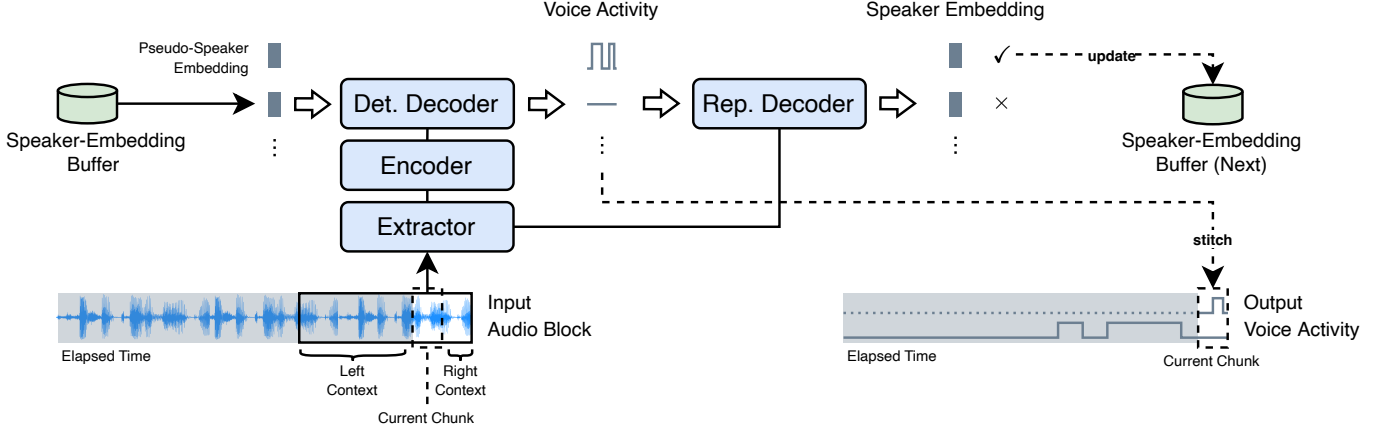


Fig. 3. The inference diagram of the Sequence-to-Sequence Neural Diarization (SSND) framework. *Det.* and *Rep.* denote the abbreviations of detection and representation, respectively.

be padded by either the non-speech embedding or randomly selected speakers not appearing in the current audio block. Accordingly, their ground-truth voice activities are silent. In this way, the input dimension of a mini-batched training data can be aligned, and the model is trained to distinguish valid and invalid speaker embeddings for the given audio block and how to assign target voice activities to the corresponding speakers.

Finally, the output $\hat{\mathbf{Y}}$ from the detection decoder is optimized to minimize its binary cross-entropy (BCE) loss with \mathbf{Y} , which is described as follows:

$$\mathcal{L}_{\text{bce}} = -\frac{1}{N \times T'} \sum_{n=1}^N \sum_{t'=1}^{T'} [y_{n,t'} \log(\hat{y}_{n,t'}) + (1 - y_{n,t'}) \log(1 - \hat{y}_{n,t'})], \quad (3)$$

where $\hat{y}_{n,t'} = \hat{\mathbf{Y}}(n, t')$ is the predicted speaking probability of the n -th speaker at time t' . And $y_{n,t'} = \mathbf{Y}(n, t')$ is its ground-truth label.

2) *Target-voice speaker embedding extraction:* As speaker embeddings can be used as reference information to extract target speaker voice activities, why can't voice activities be used as reference information to extract target speaker embeddings from multi-talker audio signals? Following this idea, we propose the target-voice speaker embedding extraction method, an inverse function of target-speaker voice activity detection.

The ArcFace [68] loss is employed between $\hat{\mathbf{E}}$ and the embedding matrix \mathbf{E}_{all} , which is described as follows:

$$\mathcal{L}_{\text{arc}} = \frac{1}{N} \sum_{n=1}^N -\log \frac{e^{s \cos(\theta_n + m)}}{e^{s \cos(\theta_n + m)} + \sum_{i=1, i \neq S_n}^{N_{\text{all}}} e^{s \cos \theta_i}}, \quad (4)$$

where θ_n is the angle between the n -th extracted speaker embedding $\hat{\mathbf{e}}_n \in \hat{\mathbf{E}}$ and its ground-truth embedding $\in \mathbf{E}_{\text{all}}$; θ_i is the angle between $\hat{\mathbf{e}}_n$ and the i -th speaker embedding $\in \mathbf{E}_{\text{all}}$. Let S_n represent the index of the n -th given speaker label corresponding to $\hat{\mathbf{e}}_n$, $i \neq S_n$ controls that θ_i is only implemented on negative pairs in such contrastive learning. s and m are the re-scale factor and additive angular margin penalty, respectively.

The total training loss is the sum of \mathcal{L}_{bce} in Eq. 3 and \mathcal{L}_{arc} in Eq. 4. Using a learnable embedding matrix as the bridge between the built-in decoders, the embedding space of speaker detection and representation can be jointly optimized in an end-to-end manner.

C. Inferring Process

Fig. 3 demonstrates the inference diagram of our proposed SSND framework. Once the training is finished, the embedding matrix will no longer be needed. Instead, a speaker-embedding buffer is initialized as an empty dictionary to store speaker embeddings extracted during inference. Then, the model processes the input audio block by block and progressively updates the speaker-embedding buffer.

1) *Data preparation:* The length of each input audio block is set to l , usually spanning several seconds to involve more contextual information. To reduce the latency of model output, we introduce a smaller unit: chunk. As shown in the left part of Fig. 3, each input audio block contains three regions: left context, current chunk, and right context. The chunk length is set to l_{chunk} , representing the period corresponding to each inference step. The lengths of left and right contexts are set to l_{left} and l_{right} , respectively. A sliding window method is applied to move the current chunk on the audio stream with the chunk shift equal to chunk length. For each inference, the model takes the input audio block containing the current chunk and its contexts as long as $l = l_{\text{left}} + l_{\text{chunk}} + l_{\text{right}}$. At the beginning of inference, absent left context can be padded with zeros until the acquired audio signal is available to compose an entire block. Furthermore, since acquiring the right context needs to await an extra period, the algorithmic latency of model inference should be the sum of l_{chunk} and l_{right} .

The input embeddings consist of three different sources. The first part is always kept for the pseudo-speaker embedding \mathbf{e}_{pse} . The second part consists of the target embeddings enrolled in the current speaker-embedding buffer. The third part is padded by the non-speech embedding \mathbf{e}_{non} . Assume that speaker capacity is set to N during training and there are currently N_{loc} identities enrolled in the speaker-embedding

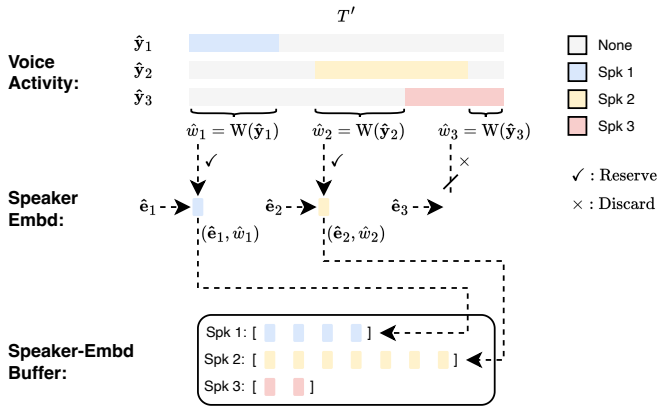


Fig. 4. Updating strategy of the speaker-embedding buffer.

buffer, the set of input embeddings can be obtained by $\mathbf{E} = \{e_{\text{pse}}\} \cup \{e_n \mid 1 \leq n \leq N_{\text{loc}}\} \cup \{e_{\text{non}}\}^{N-N_{\text{loc}}-1}$. Therefore, the inputs of both audio block and target-speaker embeddings can maintain the fixed dimensions during inference.

2) *Decoding Procedure*: The first decoding stage takes the given speaker embeddings as reference information to predict multiple speakers' voice activities from its detection decoder. As the input order of speaker embeddings determines the output order of target voice activities, the predicted target-speaker voice activities also have three parts, denoted by $\hat{\mathbf{Y}} = \{\hat{y}_{\text{pse}}\} \cup \{\hat{y}_n \mid 1 \leq n \leq N_{\text{loc}}\} \cup \{\hat{y}_{\text{non}}\}^{N-N_{\text{loc}}-1}$. Let each $\hat{y} = [y_1, y_2, \dots, y_{T'}] \in \hat{\mathbf{Y}}$ indicates a given speaker's prediction result with T' timestamps. The \hat{y}_{pse} represents the output corresponding to the pseudo-speaker embedding e_{pse} . For $\{\hat{y}_n \mid 1 \leq n \leq N_{\text{loc}}\}$, each \hat{y}_n represents the output corresponding to the target embedding e_n . Since $\{\hat{y}_{\text{non}}\}^{N-N_{\text{loc}}-1}$ belongs to the output of padded non-speech embeddings $\{e_{\text{non}}\}^{N-N_{\text{loc}}-1}$, these results are invalid.

The second decoding stage takes the predicted voice activities as reference information to extract multiple speakers' embeddings from its representation decoder. Similarly, the input order of voice activities determines the output order of target speaker embeddings. The extracted target-speaker embeddings also have three parts, denoted by $\hat{\mathbf{E}} = \{\hat{e}_{\text{pse}}\} \cup \{\hat{e}_n \mid 1 \leq n \leq N_{\text{loc}}\} \cup \{\hat{e}_{\text{non}}\}^{N-N_{\text{loc}}-1}$. As the quality of embedding extraction may be easily affected by each speaker's active speaking time and overlapping status, we define the operation $W(\hat{y}) = \sum_{t'=1, t' \notin \text{Overlap}}^{T'} y_{t'}$ to count the non-overlapped speaking time in the given \hat{y} . The longer single-speaking time for each speaker usually results in better embedding extraction, which can be used as an additional embedding weight. Thus, the weights of $\hat{\mathbf{E}}$ can be denoted as $\hat{\mathbf{W}} = \{\hat{w}_{\text{pse}}\} \cup \{\hat{w}_n \mid 1 \leq n \leq N_{\text{loc}}\} \cup \{\hat{w}_{\text{non}}\}^{N-N_{\text{loc}}-1}$.

We adopt two thresholds denoted as t_1 and t_2 , respectively. If $\hat{w}_{\text{pse}} > t_1$, it means that an unenrolled speaker is detected and the extracted embedding is qualified to be reserved. The results of \hat{y}_{pse} and \hat{e}_{pse} will be assigned a new speaker label. Otherwise, \hat{y}_{pse} and \hat{e}_{pse} will be discarded as invalid results. For $\{\hat{e}_n \mid 1 \leq n \leq N_{\text{loc}}\}$, each \hat{e}_n represents the output corresponding to the target voice activity \hat{y}_n . If $\hat{w}_n > t_2$, the results of \hat{y}_n and \hat{e}_n will be reserved. Otherwise, \hat{e}_n will be discarded

Algorithm 1 Pseudocode of online inference in the Python-like style.

```

"""
Functions
- Extractor(), Encoder(), Dia_Decoder(), Emb_Decoder(): neural network
  modules in the SSND model
- W(): calculating embedding weight

Inputs
- blocks: a sequence of input audio blocks
- e_pse: pseudo-speaker embedding
- e_non: non-speech embedding
- t1: threshold for pseudo-speaker embedding weight
- t2: threshold for enrolled-speaker embedding weight
- lc: number of output VAD frames belonging to the current chunk
- lr: number of output VAD frames belonging to the right context
- N: speaker capacity
- S: embedding dimension

```

```

Outputs
- dia_result: predicted target-speaker voice activities
- emb_buffer: extracted speaker embeddings

```

```

For clarity, the batch dimension of the pytorch tensor is omitted to
describe, where it is always 1 during each inference.
"""

```

```

dia_result = {} # initial diarization result
emb_buffer = {} # initial speaker-embedding buffer
num_frames = 0 # number of predicted VAD frames

for audio_block in blocks: # load the next audio block
    # initialize lists for input speaker embeddings and labels
    emb_list = [e_pse] # put pseudo-speaker embedding
    spk_list = [len(emb_buffer)+1] # create new speaker label

    # obtain each enrolled target-speaker embedding
    for spk_id in emb_buffer.keys():
        e_sum = torch.zeros(S) # embedding vector, shape: S
        w_sum = 0 # embedding weight, scalar
        for e_i, w_i in emb_buffer[spk_id]:
            e_sum += w_i*e_i
            w_sum += w_i
        emb_list.append(e_sum/w_sum) # append weighted speaker embedding
        spk_list.append(spk_id) # append speaker label
    # pad input embeddings to tensor with the length of N
    while len(emb_list) < N:
        emb_list.append(e_non)
    emb_tensor = torch.stack(emb_list)

    # forward networks
    X = Extractor(audio_block) # output shape: T x F
    X_hat = Encoder(X) # output shape: T x D
    Y_hat = Dia_Decoder(X_hat, emb_tensor) # output shape: N x T'
    E_hat = Emb_Decoder(X, Y_hat) # output shape: N x S

    # decode the pseudo-speaker
    y_pse = Y_hat[0] # predicted voice activity, shape: T'
    e_pse = E_hat[0] # extracted embedding, shape: S
    w_pse = W(y_pse) # embedding weight: scalar
    if w_pse > t1:
        # create the elapsed result as zeros
        elapsed_y = torch.zeros(num_frames)
        # cut the current chunk result from the block output
        current_y = y_pse[-(lc+lr):-lr]
        # store diarization result & embedding-weight pair
        new_id = spk_list[0]
        dia_result[new_id] = torch.cat(elapsed_y, current_y)
        emb_buffer[new_id] = [(e_pse, w_pse)]

    # decode the enrolled speaker
    for n in range(1, len(S)):
        y_n = Y_hat[n] # predicted voice activity, shape: T'
        e_n = E_hat[n] # extracted embedding, shape: S
        w_n = W(y_n) # embedding weight, scalar
        # stitch diarization result
        spk_id = spk_list[n]
        dia_result[spk_id] = \
            torch.cat(dia_result[spk_id], y_n[-(lc+lr):-lr])
        # append embedding-weight pair
        if w_n > t2:
            emb_buffer[spk_id].append((e_n, w_n))

num_frames += lc # update

```

to prevent the unreliable speaker embedding from polluting the buffer. However, \hat{y}_n can still be adopted because it is predicted by target embeddings buffered previously. Lastly, valid results of the predicted voice activities will be stitched onto their preceding predictions in the elapsed time. It must be noticed that only the output region belonging to the current chunk can be adopted as new predictions in every inference, which ensures the temporal causality of online inference. Valid results of the extracted speaker embeddings are updated in the speaker-embedding buffer to infer the next audio block.

3) *Buffer Updating*: Fig. 4 illustrates the updating strategies for selecting and buffering target-speaker embeddings at the end of each inference. In this example, both \hat{w}_1 and \hat{w}_2 exceed the preset threshold for reserving, but \hat{w}_3 is discarded. In the dictionary-based speaker-embedding buffer, the keys represent the enrolled speaker labels, and the corresponding values contain lists of embedding-weight pairs, respectively. Each reserved speaker embedding and its weight are appended into the buffer according to the key of the speaker label. When inferring the next audio block, each speaker’s target embedding for model input will be the weighted average of all the buffered results. To formally describe this procedure, let $\{\hat{e}_n^1, \hat{e}_n^2, \dots, \hat{e}_n^{K_n}\}$ and $\{\hat{w}_n^1, \hat{w}_n^2, \dots, \hat{w}_n^{K_n}\}$ denote the embeddings and weights of the n -th speaker in the buffer, where K_n is the number of embeddings. The aggregation of target-speaker embedding can be calculated as follows:

$$\bar{e}_n = \frac{\sum_{k=1}^{K_n} (\hat{w}_n^k \cdot \hat{e}_n^k)}{\sum_{k=1}^{K_n} \hat{w}_n^k}. \quad (5)$$

Algorithm 1 summarizes the pseudocode of online inference in a Python-like style. A live audio signal can be fed into the proposed model by a sliding window approach. The neural network detects if a new speaker appears in each coming audio block by itself, eliminating the use of any prior system (e.g., the cascaded diarization). Then, it finishes the target-speaker voice activity detection and embedding extraction for the following audio blocks. In such blockwise processing, the predictions are output immediately as an online diarization system.

In addition, our proposed framework can achieve better performance through a rescoring mechanism. After the online inference, the speaker-embedding buffer will collect all target-speaker embeddings from the full audio recording. If intermediate features of the extractor and encoder are cached during the first-pass inference, the final speaker-embedding buffer can be used to fastly re-decode the audio, which acts as an offline diarization system. Beneficial to the co-designed training and inferring techniques, our proposed framework adapts to both online and offline inference modes.

IV. EXPERIMENTAL SETTINGS

A. Datasets

To train the SSND models with numerous speaker identities, we introduce two speaker corpora for data simulation. The first corpus is the widely-used VoxCeleb2 [69] with over 1 million utterances for 6,112 identities. The second corpus is the recently released VoxBlink2 [70] with approximately 10 million utterances for 111,284 identities. We employ the FSMN-VAD module in FunASR [71] toolkit to remove non-speech regions from the raw audio, purifying the data as much as possible. Then, the simulated data is generated in an on-the-fly manner during training. First, the single-speaker utterance is independently created by alternately concatenating the source speech and silent (zero-padded) segments, where each segment length is randomly sampled from a uniform distribution of 0-4 seconds. Second, we randomly mix utterances

TABLE I
STATISTICS OF DATASETS USED IN OUR EXPERIMENTS. THE OVERLAP RATIOS OF SIMULATED DATA ARE ESTIMATED ON 250,000 RANDOMLY GENERATED SAMPLES.

Dataset	Split	Num. Speakers	Num. Recordings	Overlap Ratio
On-the-fly Simulation	sim1spk	1	-	0.00%
	sim2spk	2	-	28.01%
	sim3spk	3	-	39.66%
	total	1-3	-	22.56%
DIHARD-II [72]	dev153	1-10	153	9.78%
	dev39	1-9	39	9.73%
	eval	1-9	194	8.90%
DIHARD-III [73]	dev203	1-10	203	10.83%
	dev51	1-8	51	10.37%
	eval	1-9	259	9.37%

of 1-3 speakers from the corpora, which follows the same implementation in our previous works [13], [52].

The models pretrained by simulated data are further adapted and evaluated on real multi-domain datasets: DIHARD-II [72] and DIHARD-III [73], respectively. The DIHARD-II dataset includes 11 conversational scenarios (e.g., interview, clinical, restaurant), with 23.81 hours of development set and 22.49 hours of evaluation set. We select the first 153 recordings (80%) of the original development set for model adaptation, namely the *dev153* set. The last 39 recordings (20%) remain for validation, namely the *dev39* set. The DIHARD-III dataset is the next edition of the DIHARD-II dataset in a series of speaker diarization challenges, with 34.15 hours of development set and 33.01 hours of evaluation set. Similarly, we select the first 203 recordings (80%) of the original development set for model adaptation, namely the *dev203* set. The last 51 recordings (20%) remain for validation, namely the *dev51* set. The statistics of both simulated and real datasets are described in Table I.

B. Network Configurations

1) *Pretrained extractor*: As the pretrained front-end extractor can effectively facilitate the model to learn the identity information in target-speaker embeddings, we pretrain three speaker embedding extractors with similar network architecture but different model sizes and training data. The first two extractors are both based on the ResNet-34 model, while their residual blocks have respective channels of $\{32, 64, 128, 256\}$ and $\{64, 128, 256, 512\}$, namely the ResNet34-32ch and ResNet34-64ch. After adding the global statistical pooling (GSP) [32] and linear projection layer with the output dimension of 256, these two extractors are trained on the VoxCeleb2 [69] dataset by the ArcFace ($s = 32, m = 0.2$) [68] classifier. We also introduce the third ResNet-152 model trained on the VoxBlink2 [70] dataset to explore the potential of large model size and training data. The ResNet34-32ch, ResNet34-64ch, and ResNet-152 models have 5.45M, 21.53M, and 58.14M parameters, respectively. Accordingly, they obtain 1.17%, 0.81%, and 0.34% equal error rates (EERs) on the Vox-O [74] trial.

2) *SSND model*: For the entire SSND model, we propose two versions with different numbers of parameters. The first is named SSND-Small. Its extractor is based on the ResNet34-32ch model. The following encoder and decoder adopt 256-dim attentions with 8 heads and 512-dim feedforward layers. The second is named SSND-Medium. Its extractor is based on the ResNet34-64ch model. The encoder and decoder are changed to 384-dim attentions with 8 heads and 768-dim feedforward layers. The other configurations for the two models are identical. All encoders and decoders have 4 blocks. The kernel size of convolutions in Conformer blocks is set to 15. In total, the parameters in the SSND-Small and SSND-Medium models are 16.56M and 45.96M, respectively. Because the heavy parameters in the ResNet-152 extractor are unsuitable for online inference, we only use it as the teacher model of knowledge distillation [75] to improve the current models described in the next paragraph.

C. Training and Inferring Details

1) *Training details*: All training audio is split into fixed-length blocks and normalized with a mean of 0 and a standard deviation of 1. Specifically, the block length in this work is set to 8 seconds. The input acoustic features are 80-dim log Mel-filterbank energies with a frame length of 25 ms and a shift of 10 ms. Also, we apply the additive noise from Musan [76] and reverberation from RIRs [77] as audio augmentation. As suggested by our previous findings [13], [52], the temporal resolution (duration per frame-level prediction) of system output is directly set to 10 ms for precise option. The speaker capacity N is adopted as 30, a relatively large number that can adequately cover the maximum number of speakers in most datasets.

When the number of speakers in a given audio block cannot reach N , absent positions will be padded as described in Sec. III-B1. Lastly, all the input target-speaker embeddings are randomly shuffled to make the model invariant to speaker order. Accordingly, the ground truth labels for target-speaker voice activity detection and embedding extraction must also be re-assigned based on their shuffled results. Then, the whole model is optimized by AdamW [78] optimizer with the binary cross entropy (BCE) loss and ArcFace ($s = 32, m = 0.2$) [68] loss depicted in Fig. 1. Using $8 \times$ NVIDIA RTX-3090 GPUs with a batch size of 16, we investigate two multi-stage training strategies as follows.

The first training strategy follows our previous work [13], containing three different stages starting from the pretrained extractor. In each stage, the model will be validated every 500 steps. The checkpoint with the lowest diarization error rate on the adopted validation set will be used for the next stage.

- Stage 1: We copy and freeze the weights of a pretrained speaker embedding model to initialize the front-end extractor. Only simulated data is used to train the back-end modules for 100,000 steps with a learning rate of $1e-4$.
- Stage 2: The front-end extractor is unfrozen. The whole SSND model is adapted by 80% of the simulated data and 20% of the real data from the specific dataset, taking around 75,000 steps.

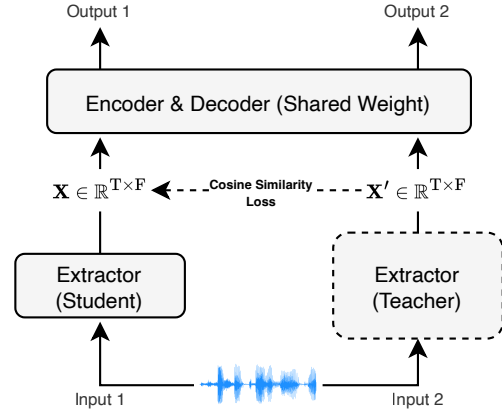


Fig. 5. Illustration of the training strategy based on knowledge distillation.

- Stage 3: The learning rate is decayed to $1e-5$ for finetuning the whole SSND model, taking around 50,000 steps.

In this work, we also explore the second kind of training strategy based on knowledge distillation, shown in Fig. 5. The pretrained ResNet-152 model is employed as the teacher extractor. The original input audio will be copied to feed the student and teacher extractors during training. Let $\mathbf{X} = [\mathbf{x}_1, \dots, \mathbf{x}_T] \in \mathbb{R}^{T \times F}$ denote the output of the student extractor, where T is the time axis and F is the feature axis. Comparatively, the output of the teacher extractor is represented as $\mathbf{X}' = [\mathbf{x}'_1, \dots, \mathbf{x}'_T] \in \mathbb{R}^{T \times F}$. Then, we employ a frame-wise cosine similarity loss between two extractors, which is described as:

$$\mathcal{L}_{\text{distill}} = 1 - \frac{1}{T} \sum_{t=1}^T \frac{\mathbf{x}_t \cdot \mathbf{x}'_t}{\|\mathbf{x}_t\| \cdot \|\mathbf{x}'_t\|}, \quad (6)$$

where \mathbf{x}_t and $\mathbf{x}'_t \in \mathbb{R}^F$ represent the frame-level speaker embedding extracted by the student and teacher extractors at time t , respectively. By minimizing $\mathcal{L}_{\text{distill}}$, the representation space of \mathbf{X} is forced to align with \mathbf{X}' , which means the knowledge in the larger teacher extractor transfers into the smaller student extractor. Later, \mathbf{X} and \mathbf{X}' are fed into the shared encoder and decoder modules as same as the regular training framework described in Sec. III-B. The original ground-truth labels are also copied to supervise the two output branches. There are also three training stages, similar to the pretraining strategy.

- Stage 1: We initialize the weights of the student extractor from scratch and freeze the pretrained teacher extractor. Only simulated data is used to train the student extractor and back-end modules for 100,000 steps with a learning rate of $1e-4$.
- Stage 2: The teacher extractor is unfrozen. The whole SSND model is adapted by 80% of the simulated data and 20% of the real data from the specific dataset, taking around 75,000 steps.
- Stage 3: The learning rate is decayed to $1e-5$ for finetuning the whole SSND model, taking around 50,000 steps.

2) *Inferring details*: The inferring process follows the Sec. III-C. The thresholds t_1 and t_2 are determined using grid search on the validation set of the specific dataset. By adjusting

TABLE II

PERFORMANCE OF SSND MODELS ON DIHARD-II AND DIHARD-III EVALUATION SETS WITH VARIOUS TRAINING AND INFERRING CONDITIONS. THE DIARIZATION ERROR RATES (DERs) ARE REPORTED WITHOUT ORACLE VAD AND COLLAR TOLERANCE.

ID	Model Size	Simulation Corpus	Training Strategy	Chunk Length	Right-Context Length	Algorithmic Latency	DIHARD-II Eval		DIHARD-III Eval	
							Online DER (%)	Offline DER (%)	Online DER (%)	Offline DER (%)
S1	Small	VoxCeleb2	Pretraining	0.48s	-	0.48s	27.79	23.74	20.55	16.28
S2				0.48s	0.16s	0.64s	26.11	23.85	18.53	16.33
S3				0.64s	-	0.64s	27.54	24.07	19.72	16.36
S4				0.64s	0.16s	0.80s	25.79	23.52	18.33	16.33
S5	Small	VoxBlink2	Pretraining	0.48s	-	0.48s	27.39	22.80	20.45	16.51
S6				0.48s	0.16s	0.64s	25.72	22.97	18.44	16.38
S7				0.64s	-	0.64s	26.93	23.05	19.55	16.32
S8				0.64s	0.16s	0.80s	25.70	23.17	18.36	16.45
S9	Small	VoxBlink2	Distillation	0.48s	-	0.48s	27.87	23.88	21.33	17.70
S10				0.48s	0.16s	0.64s	26.71	24.36	19.42	17.51
S11				0.64s	-	0.64s	27.58	24.28	20.67	17.57
S12				0.64s	0.16s	0.80s	26.21	24.29	19.23	17.57
S13	Medium	VoxCeleb2	Pretraining	0.48s	-	0.48s	27.57	23.78	20.61	16.81
S14				0.48s	0.16s	0.64s	25.57	23.61	18.82	16.97
S15				0.64s	-	0.64s	27.00	23.83	20.08	16.83
S16				0.64s	0.16s	0.80s	25.78	23.89	18.43	16.79
S17	Medium	VoxBlink2	Pretraining	0.48s	-	0.48s	27.79	24.09	20.13	16.04
S18				0.48s	0.16s	0.64s	26.02	23.86	18.10	15.77
S19				0.64s	-	0.64s	27.10	23.77	19.30	15.83
S20				0.64s	0.16s	0.80s	25.55	23.59	17.99	15.93
S21	Medium	VoxBlink2	Distillation	0.48s	-	0.48s	26.13	21.95	19.11	15.14
S22				0.48s	0.16s	0.64s	24.41	22.17	17.33	15.30
S23				0.64s	-	0.64s	25.44	22.07	18.46	15.13
S24				0.64s	0.16s	0.80s	24.48	22.26	17.12	15.23

The lowest online and offline DERs of each model size are highlighted by the gray background.

the proportion of the current chunk and its contexts in the input audio block, the online diarization system can be flexibly inferred at different latencies. The algorithmic latency is the sum of chunk length l_{chunk} and right-context length l_{right} . As the shift of the sliding window is equal to the chunk length, a smaller l_{chunk} can decrease the system latency but bring intensive computing. The right context represents the use of future information. A larger l_{right} may result in more accurate prediction but increase the system latency. The impacts of different settings are investigated in the experimental results.

D. Evaluation Metric

The diarization error rate (DER) is used as the evaluation metric without collar tolerance. The SSND models are tested on evaluation sets of DIHARD-II [72] and DIHARD-III [73] datasets. For a fair comparison, the Oracle VAD information can revise the diarization results as a post-processing approach [10] if sometimes the evaluation condition allows.

V. RESULTS

A. Evaluation of SSND Models

Table II illustrates the performance of our proposed SSND models with different training and inferring conditions. The effects of model size, simulation corpus, training strategy, and various combinations of chunk and right-context lengths are shown step by step. Browsing the DER results on DIHARD-II

and DIHARD-III datasets, several consequences can be found as follows.

- 1) Comparing *S1-4*, the increase in algorithmic latency leads to lower online DERs. Especially, using right-context information can bring significant improvement than not using it, even if the total latency is the same between *S2* and *S3*. However, their offline DERs do not exhibit apparent gaps. As the rescoring mechanism updates the diarization output over the whole recording, the offline performance is insensitive to the latency of the first-pass online inference. These phenomena are also shown in all the other experimental groups.
- 2) Comparing *S1-4*, *S5-8*, and *S9-12*, we evaluate the small model with different simulation corpora and training strategies. It can be seen that the VoxBlink2 corpus containing larger speaker identities (111k+) does not result in significant and consistent improvement over VoxCeleb2 (6k+). Also, the training strategy of knowledge distillation slightly downgrades the performance compared to the pretraining strategy. It is speculated that the small model with few parameters cannot fully exploit the large simulation corpus and knowledge distillation.
- 3) Comparing *S13-16*, *S17-20* and *S21-24*, we evaluate the medium model with different simulation corpora and training strategies again. In this case, the combination of VoxBlink2 corpus and knowledge distillation demonstrates overwhelming advantages over others. All

TABLE III
COMPARISONS OF SSND MODELS WITH OTHERS ON THE DIHARD-II
EVALUATION SET.

Method	Latency (s)	DER (%)
Online		
EEND-EDA + FW-STB [24]	1.00	36.00
EEND-EDA + Improved FW-STB [25]	1.00	33.37
Overlap-aware Speaker Embeddings [58]	1.00	35.10
EEND-GLA-Small + BW-STB [25]	1.00	31.47
EEND-GLA-Large + BW-STB [25]	1.00	30.24
SSND-Small (S8 in Table II)	0.80	25.70
SSND-Medium (S22 in Table II)	0.64	24.41
Online (with oracle voice activity detection)		
UIS-RNN-SML [57]	1.00	27.30
EEND-EDA + FW-STB [24]	1.00	25.80
EEND-EDA + Improved FW-STB [25]	1.00	24.67
Core Samples Selection [79]	1.00	23.10
EEND-GLA-Small + BW-STB [25]	1.00	23.26
EEND-GLA-Large + BW-STB [25]	1.00	21.92
NAVER System [80]	0.50	21.60
SSND-Small (S8 in Table II) + Oracle VAD	0.80	18.07
SSNDD-Medium (S22 in Table II) + Oracle VAD	0.64	18.65
Offline		
EEND-EDA [10]		29.57
+ Iterative Inference+ [10]		28.52
EEND-GLA-Small [25]		29.31
EEND-GLA-Large [25]		28.33
BUT System [33] †		27.11
+ EEND Post-Processing [81]		26.88
AED-EEND [82]		25.92
+ Embedding Enhancer [82]		24.64
SSND-Small (S5 in Table II)		22.80
SSND-Medium (S21 in Table II)		21.95
Offline (with oracle voice activity detection)		
EEND-EDA [10]		20.54
+ Iterative Inference+ [10]		20.24
VBx [5]		18.55
BUT System [33] †		18.42
SSND-Small (S5 in Table II) + Oracle VAD		15.84
SSND-Medium (S21 in Table II) + Oracle VAD		15.34

† Winning system on Track 1&2 of the DIHARD-II Challenge.

the lowest DERs for medium model on two datasets are obtained in *S21-24*. When increasing the number of model parameters, the newly introduced distillation strategy can successfully empower the usage of large speaker identities in the simulation corpus.

Overall, for the SSND-Small model, the best online DERs on DIHARD-II and DIHARD-III datasets are 25.70% and 18.33%, and the best offline DERs on the two datasets are 22.80% and 16.28%, respectively. For the SSND-Medium model, the best online DERs on DIHARD-II and DIHARD-III datasets are 24.41% and 17.12%, and the best offline DERs on two datasets are 21.95% and 15.13%, respectively. To summarize, the combination of a small simulation corpus and pretraining strategy is the better choice for the small model. When a large simulation corpus is available, adopting the medium model and distillation strategy can achieve better DER performance.

B. Comparison with Other Existing Methods

We select the lowest online and offline DERs for each model size on DIHARD-II and DIHARD-III datasets as the representative results, highlighted by the gray background in

TABLE IV
COMPARISONS OF SSND MODELS WITH OTHERS ON THE DIHARD-III
EVALUATION SET.

Method	Latency (s)	DER (%)
Online		
Overlap-aware Speaker Embeddings [58]	1.00	27.60
EEND-EDA + Improved FW-STB [25]	1.00	25.09
EEND-GLA-Small + BW-STB [25]	1.00	22.00
EEND-GLA-Large + BW-STB [25]	1.00	20.73
ResNet-based OTS-VAD [27]	0.80	19.07
SSND-Small (S4 in Table II)	0.80	18.33
SSND-Medium (S24 in Table II)	0.80	17.12
Online (with oracle voice activity detection)		
Zhang et al. [20]	0.50	19.57
Core Samples Selection [79]	1.00	19.30
NAVER System [80]	0.50	19.05
EEND-EDA + Improved FW-STB [25]	1.00	18.58
EEND-GLA-Small + BW-STB [25]	1.00	15.82
EEND-GLA-Large + BW-STB [25]	1.00	14.70
ResNet-based OTS-VAD [27]	0.80	13.31
SSND-Small (S4 in Table II) + Oracle VAD	0.80	13.07
SSND-Medium (S24 in Table II) + Oracle VAD	0.80	11.88
Offline		
EEND-EDA [10]		21.55
+ Iterative Inference+ [10]		20.69
Pyannote.audio v3.1 [83]		21.30
DiaPer [42]		20.30
EEND-GLA-Small [25]		20.23
EEND-GLA-Large [25]		19.49
VBx + Overlap-aware Resegmentation [34]		19.30
USTC-NELSLIP System [14] †		16.78
ANSD-MA-MSE [84]		16.76
EEND-M2F [85]		16.07
SSND-Small (S1 in Table II)		16.28
SSND-Medium (S23 in Table II)		15.13
Offline (with oracle voice activity detection)		
EEND-EDA [10]		14.91
+ Iterative Inference+ [10]		14.42
Hitachi-JHU System [86]		11.58
USTC-NELSLIP System [14] †		11.30
ANSD-MA-MSE [84]		11.12
Seq2Seq-TSVAD [13]		10.77
MIMO-TSVAD [52]		10.10
SSND-Small (S1 in Table II) + Oracle VAD		11.13
SSND-Medium (S23 in Table II) + Oracle VAD		10.37

† Winning (fusion) system on Track 1&2 of the DIHARD-III Challenge.

Table II. To fairly compare with some existing methods, the corresponding results of post-processing by Oracle VAD [10] are also provided.

Table III compares our proposed methods with the previous state-of-the-art results on the DIHARD-II dataset. In the online scenario, our proposed methods obtain the lowest DERs of 18.07% and 24.41% with and without Oracle VAD, respectively. Regarding algorithmic latency, our proposed methods still have a significant advantage over others when Oracle VAD is not used. In the offline scenario, our proposed methods obtain the lowest DERs of 15.34% and 21.95% with and without Oracle VAD, respectively. Generally, our best results significantly outperform previous state-of-the-art systems in all scenarios. Notably, our best online DER (24.41%) is even lower than the previous best offline system (24.64%) [82] and the winning system (27.11%) [33] of the DIHARD-II Challenge.

Table IV compares our proposed methods with the previous state-of-the-art results on the DIHARD-III dataset. In the

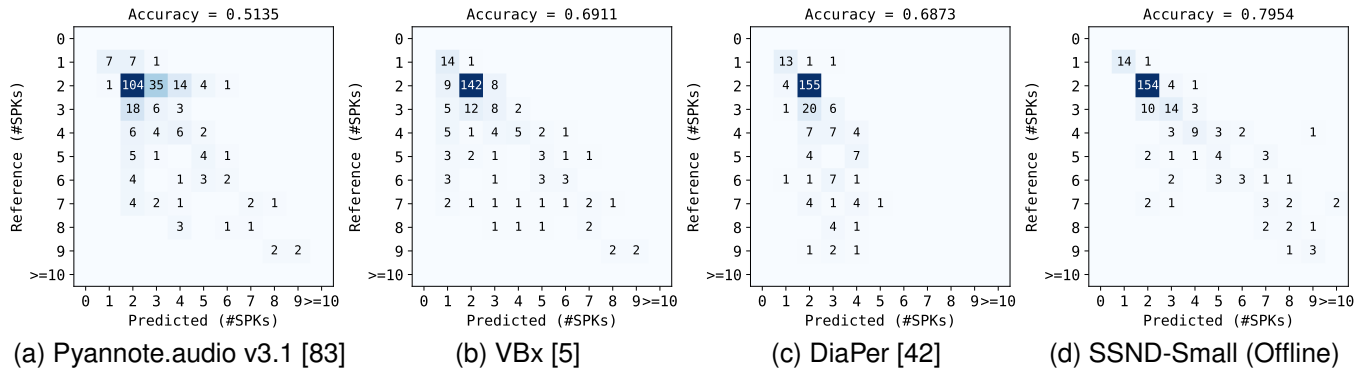


Fig. 6. Confusion matrices for speaker counting on the DIHARD-III evaluation set. The Pyannote.audio v3.1, VBx, and DiaPer results are provided by their respective authors. For our trained SSND-Small model, the same settings as S_4 in Table II are adopted. Oracle VAD is not used.

online scenario, our proposed methods obtain the lowest DERs of 11.88% and 17.12% with and without Oracle VAD, respectively. In the offline scenario, our proposed methods obtain the lowest DERs of 10.37% and 15.13% with and without Oracle VAD, respectively. Except for the offline result with Oracle VAD, our best results significantly outperform previous state-of-the-art systems in all other scenarios. Nevertheless, the DER (10.10%) of MIMO-TSVAD [52] comes from our earlier study designed for offline scenarios, which adopts the audio block of 32 seconds to provide extended context but is not suitable for online inference. Last but not least, our best online DER (17.12%) is very close to the previous best offline system (16.07%) [85] and the winning fusion system (16.78%) [14] of the DIHARD-III Challenge.

C. Investigation of Speaker Counting Ability

The previous speaker diarization systems mainly utilize unsupervised clustering [3]–[6], permutation-invariant training [7]–[10], or their combination to determine the unknown number of speakers in the input audio. In our proposed SSND framework, speakers can be found by traversing the entire audio using the masked speaker prediction mechanism, which is clustering-free. Also, it only adds one unknown speaker each time to avoid the increasing complexity problem of the permutation-invariant training.

Fig. 6 depicts the confusion matrices for speaker counting obtained by different methods on the DIHARD-III evaluation set. Due to space limitations, only offline performances without Oracle VAD are shown. We select three representative systems from different technical routes for comparison. The first Pyannote.audio v3.1 [83] is a hybrid method of supervised end-to-end diarization and unsupervised clustering. The second VBx [5] is a well-known clustering-based diarization method, where the shown performance is reproduced as the baseline in the third EEND-based method (DiaPer [42]). As a result, the SSND-Small model exhibits the more balanced predictions with the highest accuracy of 79.54%, proving the speaker counting ability of our proposed SSND framework.

D. Computing Efficiency

Table V illustrates the computing efficiency of the SSND models. First, the total number of model parameters is an es-

TABLE V
COMPUTING EFFICIENCY REGARDING THE NUMBER OF PARAMETERS, FLOATING-POINT OPERATIONS PER SECOND (FLOPS), AND REAL-TIME FACTOR (RTF).

Model	Params (M)	FLOPS (G)	RTF
SSND-Small			
$l_{\text{chunk}} = 0.48s$	16.56	78.83	0.19
$l_{\text{chunk}} = 0.64s$	16.56	59.12	0.14
SSND-Medium			
$l_{\text{chunk}} = 0.48s$	45.96	308.89	0.22
$l_{\text{chunk}} = 0.64s$	45.96	231.67	0.15

sential measurement. Second, as mentioned in Sec IV-C2, the chunk length (l_{chunk}) determines the shift of the sliding window in our settings. Given the amount of floating-point operations for processing each window as Δ_{flops} , the Floating-Point Operations Per Second (FLOPS) is calculated as $\Delta_{\text{flops}}/l_{\text{chunk}}$. Third, the Real-time Factor (RTF) is calculated as the time to process each recording divided by the recording length, where all tests are based on the computer with Intel(R) Xeon(R) E5-2660 CPU @ 2.60GHz and NVIDIA RTX-3090 GPU. It can be seen that the computing costs of our proposed methods are not efficient enough, especially for the medium model. However, the maximum RTF of 0.22 is adequate for real-time inference. As shown in Fig. 6, the low accuracy of speaker detection is still the biggest obstacle to applying speaker diarization in real-world scenarios. Therefore, this work mainly focuses on reducing the diarization error rates at first.

Furthermore, comparing computing efficiency depends on various measurement criteria and hardware platforms. For instance, EEND-GLA-Small [25] has only 6.4M parameters. However, it additionally relies on clustering of relative speaker embeddings, which has $\mathcal{O}(n^3)$ time complexity but cannot be counted into FLOPS on the GPU device. OTS-VAD [27] employs an external VAD module to remove silent regions from the original audio signal. The preprocessing time (e.g., data I/O, VAD) is not involved in the RTFs reported by the authors. It is hard to compare different studies in those aspects fairly. Thus, this paper does not list the computing efficiency comparisons with other methods.

VI. CONCLUSIONS

This paper proposes a novel Sequence-to-Sequence Neural Diarization (SSND) framework to tackle online and offline speaker diarization in a unified model. The SSND models can automatically detect and represent an unknown number of speakers in the input audio signal using the well-designed training and inferring process. Experimental results prove that the proposed SSND framework obtains new state-of-the-art DERs across all online and offline inference scenarios. Nevertheless, the proposed models also have limitations. The large model size and computing cost still present challenges for real-time inference on edge devices without GPUs. In the future, we will further improve the current approach regarding both precision and speed, prompting speaker diarization to wide industrial applications.

REFERENCES

- [1] T. J. Park, N. Kanda, D. Dimitriadis, K. J. Han, S. Watanabe, and S. Narayanan, "A review of speaker diarization: Recent advances with deep learning," *Computer Speech & Language*, vol. 72, p. 101317, 2022.
- [2] N. Kanda, Y. Gaur, X. Wang, Z. Meng, Z. Chen, T. Zhou, and T. Yoshioka, "Joint speaker counting, speech recognition, and speaker identification for overlapped speech of any number of speakers," in *Proc. INTERSPEECH*, 2020, pp. 36–40.
- [3] Q. Wang, C. Downey, L. Wan, P. A. Mansfield, and I. L. Moreno, "Speaker diarization with lstm," in *Proc. ICASSP*, 2018, pp. 5239–5243.
- [4] Q. Lin, R. Yin, M. Li, H. Bredin, and C. Barras, "Lstm based similarity measurement with spectral clustering for speaker diarization," in *Proc. INTERSPEECH*, 2019, pp. 366–370.
- [5] F. Landini, J. Profant, M. Diez, and L. Burget, "Bayesian hmm clustering of x-vector sequences (vbx) in speaker diarization: Theory, implementation and analysis on standard tasks," *Computer Speech & Language*, vol. 71, p. 101254, 2022.
- [6] W. Wang, Q. Lin, D. Cai, and M. Li, "Similarity measurement of segment-level speaker embeddings in speaker diarization," *IEEE/ACM Transactions on Audio, Speech, and Language Processing*, vol. 30, pp. 2645–2658, 2022.
- [7] Y. Fujita, N. Kanda, S. Horiguchi, K. Nagamatsu, and S. Watanabe, "End-to-end neural speaker diarization with permutation-free objectives," in *Proc. INTERSPEECH*, 2019, pp. 4300–4304.
- [8] Y. Fujita, N. Kanda, S. Horiguchi, Y. Xue, K. Nagamatsu, and S. Watanabe, "End-to-end neural speaker diarization with self-attention," in *Proc. ASRU*, 2019, pp. 296–303.
- [9] S. Horiguchi, Y. Fujita, S. Watanabe, Y. Xue, and K. Nagamatsu, "End-to-end speaker diarization for an unknown number of speakers with encoder-decoder based attractors," in *Proc. INTERSPEECH*, 2020, pp. 269–273.
- [10] S. Horiguchi, Y. Fujita, S. Watanabe, Y. Xue, and P. García, "Encoder-decoder based attractors for end-to-end neural diarization," *IEEE/ACM Transactions on Audio, Speech, and Language Processing*, vol. 30, pp. 1493–1507, 2022.
- [11] J. R. Hershey, Z. Chen, J. Le Roux, and S. Watanabe, "Deep clustering: Discriminative embeddings for segmentation and separation," in *Proc. ICASSP*, 2016, pp. 31–35.
- [12] I. Medennikov, M. Korenevsky, T. Prisyach, Y. Khokhlov, M. Korenevskaya, I. Sorokin, T. Timofeeva, A. Mitrofanov, A. Andrusenko, I. Podluzhny, A. Laptev, and A. Romanenko, "Target-speaker voice activity detection: A novel approach for multi-speaker diarization in a dinner party scenario," in *Proc. INTERSPEECH*, 2020, pp. 274–278.
- [13] M. Cheng, W. Wang, Y. Zhang, X. Qin, and M. Li, "Target-speaker voice activity detection via sequence-to-sequence prediction," in *Proc. ICASSP*, 2023, pp. 1–5.
- [14] Y. Wang, M. He, S. Niu, L. Sun, T. Gao, X. Fang, J. Pan, J. Du, and C.-H. Lee, "Ustc-nelslip system description for dihard-iii challenge," *arXiv preprint arXiv:2103.10661*, 2021.
- [15] W. Wang, D. Cai, Q. Lin, L. Yang, J. Wang, J. Wang, and M. Li, "The dku-dukece-lenovo system for the diarization task of the 2021 voxceleb speaker recognition challenge," *arXiv preprint arXiv:2109.02002*, 2021.
- [16] W. Wang, X. Qin, M. Cheng, Y. Zhang, K. Wang, and M. Li, "The dku-dukecece diarization system for the voxceleb speaker recognition challenge 2022," *arXiv preprint arXiv:2210.01677*, 2022.
- [17] M. Cheng, W. Wang, X. Qin, Y. Lin, N. Jiang, G. Zhao, and M. Li, "The dku-msxf diarization system for the voxceleb speaker recognition challenge 2023," in *Proc. NCMMS*, J. Jia, Z. Ling, X. Chen, Y. Li, and Z. Zhang, Eds. Springer Nature Singapore, 2024, pp. 330–337.
- [18] J. Huh, J. S. Chung, A. Nagrani, A. Brown, J.-w. Jung, D. Garcia-Romero, and A. Zisserman, "The voxceleb speaker recognition challenge: A retrospective," *IEEE/ACM Transactions on Audio, Speech, and Language Processing*, vol. 32, pp. 3850–3866, 2024.
- [19] D. Dimitriadis and P. Fousek, "Developing on-line speaker diarization system," in *Proc. INTERSPEECH*, 2017, pp. 2739–2743.
- [20] Y. Zhang, Q. Lin, W. Wang, L. Yang, X. Wang, J. Wang, and M. Li, "Low-latency online speaker diarization with graph-based label generation," in *Proc. Odyssey*, 2022.
- [21] E. Han, C. Lee, and A. Stolcke, "Bw-eda-eend: streaming end-to-end neural speaker diarization for a variable number of speakers," in *Proc. ICASSP*, 2021, pp. 7193–7197.
- [22] D. Liang, N. Shao, and X. Li, "Frame-wise streaming end-to-end speaker diarization with non-autoregressive self-attention-based attractors," in *Proc. ICASSP*, 2024, pp. 10521–10525.
- [23] Y. Xue, S. Horiguchi, Y. Fujita, S. Watanabe, P. García, and K. Nagamatsu, "Online end-to-end neural diarization with speaker-tracing buffer," in *Proc. SLT*, 2021, pp. 841–848.
- [24] Y. Xue, S. Horiguchi, Y. Fujita, Y. Takashima, S. Watanabe, L. P. G. Perera, and K. Nagamatsu, "Online streaming end-to-end neural diarization handling overlapping speech and flexible numbers of speakers," in *Proc. INTERSPEECH*, 2021, pp. 3116–3120.
- [25] S. Horiguchi, S. Watanabe, P. García, Y. Takashima, and Y. Kawaguchi, "Online neural diarization of unlimited numbers of speakers using global and local attractors," *IEEE/ACM Transactions on Audio, Speech, and Language Processing*, vol. 31, pp. 706–720, 2023.
- [26] W. Wang, M. Li, and Q. Lin, "Online target speaker voice activity detection for speaker diarization," in *Proc. INTERSPEECH*, 2022, pp. 1441–1445.
- [27] W. Wang and M. Li, "End-to-end online speaker diarization with target speaker tracking," *arXiv preprint arXiv:2310.08696*, 2023.
- [28] S.-Y. Chang, B. Li, G. Simko, T. N. Sainath, A. Tripathi, A. van den Oord, and O. Vinyals, "Temporal modeling using dilated convolution and gating for voice-activity-detection," in *Proc. ICASSP*, 2018, pp. 5549–5553.
- [29] M. Hruz and Z. Zajc, "Convolutional neural network for speaker change detection in telephone speaker diarization system," in *Proc. ICASSP*, 2017, pp. 4945–4949.
- [30] G. Sell, D. Snyder, A. McCree, D. Garcia-Romero, J. Villalba, M. Maciejewski, V. Manohar, N. Dehak, D. Povey, S. Watanabe, and S. Khudanpur, "Diarization is hard: Some experiences and lessons learned for the jhu team in the inaugural dihard challenge," in *Proc. INTERSPEECH*, 2018, pp. 2808–2812.
- [31] N. Dehak, P. J. Kenny, R. Dehak, P. Dumouchel, and P. Ouellet, "Front-end factor analysis for speaker verification," *IEEE Transactions on Audio, Speech, and Language Processing*, vol. 19, no. 4, pp. 788–798, 2011.
- [32] D. Snyder, D. Garcia-Romero, G. Sell, D. Povey, and S. Khudanpur, "X-vectors: Robust dnn embeddings for speaker recognition," in *Proc. ICASSP*, 2018, pp. 5329–5333.
- [33] F. Landini, S. Wang, M. Diez, L. Burget, P. Matějka, K. Žmolková, L. Mošner, A. Silnova, O. Plchot, O. Novotný, H. Zeinali, and J. Rohdin, "But system for the second dihard speech diarization challenge," in *Proc. ICASSP*, 2020, pp. 6529–6533.
- [34] H. Bredin and A. Laurent, "End-to-end speaker segmentation for overlap-aware resegmentation," in *Proc. INTERSPEECH*, 2021, pp. 3111–3115.
- [35] Y. Takashima, Y. Fujita, S. Watanabe, S. Horiguchi, P. García, and K. Nagamatsu, "End-to-end speaker diarization conditioned on speech activity and overlap detection," in *Proc. SLT*, 2021, pp. 849–856.
- [36] K. Kinoshita, M. Delcroix, and N. Tawara, "Integrating end-to-end neural and clustering-based diarization: Getting the best of both worlds," in *Proc. ICASSP*, 2021, pp. 7198–7202.
- [37] —, "Advances in integration of end-to-end neural and clustering-based diarization for real conversational speech," in *Proc. INTERSPEECH*, 2021, pp. 3565–3569.
- [38] K. Kinoshita, M. Delcroix, and T. Iwata, "Tight integration of neural- and clustering-based diarization through deep unfolding of infinite gaussian mixture model," in *Proc. ICASSP*, 2022, pp. 8382–8386.
- [39] S. Horiguchi, S. Watanabe, P. García, Y. Xue, Y. Takashima, and Y. Kawaguchi, "Towards neural diarization for unlimited numbers of speakers using global and local attractors," in *Proc. ASRU*, 2021, pp. 98–105.

- [40] M. Rybicka, J. Villalba, N. Dehak, and K. Kowalczyk, "End-to-end neural speaker diarization with an iterative refinement of non-autoregressive attention-based attractors," in *Proc. INTERSPEECH*, 2022, pp. 5090–5094.
- [41] Y. Fujita, T. Komatsu, R. Scheibler, Y. Kida, and T. Ogawa, "Neural diarization with non-autoregressive intermediate attractors," in *Proc. ICASSP*, 2023, pp. 1–5.
- [42] F. Landini, M. Diez, T. Stafylakis, and L. Burget, "Diaper: End-to-end neural diarization with perceiver-based attractors," *IEEE/ACM Transactions on Audio, Speech, and Language Processing*, vol. 32, pp. 3450–3465, 2024.
- [43] Y.-R. Jeoung, J.-Y. Yang, J.-H. Choi, and J.-H. Chang, "Improving transformer-based end-to-end speaker diarization by assigning auxiliary losses to attention heads," in *Proc. ICASSP*, 2023, pp. 1–5.
- [44] D. Palzer, M. Maciejewski, and E. Fosler-Lussier, "Improving neural diarization through speaker attribute attractors and local dependency modeling," in *Proc. ICASSP*, 2024, pp. 11 911–11 915.
- [45] Y. Dissen, F. Kreuk, and J. Keshet, "Self-supervised speaker diarization," in *Proc. INTERSPEECH*, 2022, pp. 4013–4017.
- [46] Y. Takashima, Y. Fujita, S. Horiguchi, S. Watanabe, L. P. G. Perera, and K. Nagamatsu, "Semi-supervised training with pseudo-labeling for end-to-end neural diarization," in *Proc. INTERSPEECH*, 2021, pp. 3096–3100.
- [47] M. He, D. Raj, Z. Huang, J. Du, Z. Chen, and S. Watanabe, "Target-speaker voice activity detection with improved i-vector estimation for unknown number of speaker," in *Proc. INTERSPEECH*, 2021, pp. 3555–3559.
- [48] C.-Y. Cheng, H.-S. Lee, Y. Tsao, and H.-M. Wang, "Multi-target extractor and detector for unknown-number speaker diarization," *IEEE Signal Processing Letters*, vol. 30, pp. 638–642, 2023.
- [49] D. Wang, X. Xiao, N. Kanda, T. Yoshioka, and J. Wu, "Target speaker voice activity detection with transformers and its integration with end-to-end neural diarization," in *Proc. ICASSP*, 2023, pp. 1–5.
- [50] W. Wang, X. Qin, and M. Li, "Cross-channel attention-based target speaker voice activity detection: Experimental results for the m2met challenge," in *Proc. ICASSP*, 2022, pp. 9171–9175.
- [51] M. Cheng, H. Wang, Z. Wang, Q. Fu, and M. Li, "The whu-alibaba audio-visual speaker diarization system for the misp 2022 challenge," in *Proc. ICASSP*, 2023, pp. 1–2.
- [52] M. Cheng and M. Li, "Multi-input multi-output target-speaker voice activity detection for unified, flexible, and robust audio-visual speaker diarization," *arXiv preprint arXiv:2401.08052*, 2024.
- [53] Y. Jiang, R. Tao, Z. Chen, Y. Qian, and H. Li, "Target speech diarization with multimodal prompts," *arXiv preprint arXiv:2406.07198*, 2024.
- [54] W. Wang, D. Cai, M. Cheng, and M. Li, "Joint inference of speaker diarization and asr with multi-stage information sharing," in *Proc. ICASSP*, 2024, pp. 11 011–11 015.
- [55] Z. Chen, B. Han, S. Wang, Y. Jiang, and Y. Qian, "Flow-tsvad: Target-speaker voice activity detection via latent flow matching," *arXiv preprint arXiv:2409.04859*, 2024.
- [56] A. Zhang, Q. Wang, Z. Zhu, J. Paisley, and C. Wang, "Fully supervised speaker diarization," in *Proc. ICASSP*, 2019, pp. 6301–6305.
- [57] E. Fini and A. Brutti, "Supervised online diarization with sample mean loss for multi-domain data," in *Proc. ICASSP*, 2020, pp. 7134–7138.
- [58] J. M. Coria, H. Bredin, S. Ghannay, and S. Rosset, "Overlap-aware low-latency online speaker diarization based on end-to-end local segmentation," in *Proc. ASRU*, 2021, pp. 1139–1146.
- [59] A. Sholkhov, N. Kuzmin, K. A. Lee, and E. S. Chng, "Probabilistic back-ends for online speaker recognition and clustering," in *Proc. ICASSP*, 2023, pp. 1–5.
- [60] Y. Chen, G. Cheng, R. Yang, P. Zhang, and Y. Yan, "Interrelate training and clustering for online speaker diarization," *IEEE/ACM Transactions on Audio, Speech, and Language Processing*, vol. 32, pp. 1352–1364, 2024.
- [61] Z. Dai, Z. Yang, Y. Yang, J. Carbonell, Q. Le, and R. Salakhutdinov, "Transformer-XL: Attentive language models beyond a fixed-length context," in *Proc. ACL*. Association for Computational Linguistics, 2019, pp. 2978–2988.
- [62] W. Chen, T. T. Anh, X. Zhong, and E. S. Chng, "Enhancing low-latency speaker diarization with spatial dictionary learning," in *Proc. ICASSP*, 2024, pp. 11 371–11 375.
- [63] S. Wang, Z. Chen, K. A. Lee, Y. Qian, and H. Li, "Overview of speaker modeling and its applications: From the lens of deep speaker representation learning," *arXiv preprint arXiv:2407.15188*, 2024.
- [64] K. He, X. Zhang, S. Ren, and J. Sun, "Deep residual learning for image recognition," in *Proc. CVPR*, 2016.
- [65] A. Gulati, J. Qin, C.-C. Chiu, N. Parmar, Y. Zhang, J. Yu, W. Han, S. Wang, Z. Zhang, Y. Wu, and R. Pang, "Conformer: Convolution-augmented transformer for speech recognition," in *Proc. INTERSPEECH*, 2020, pp. 5036–5040.
- [66] A. Vaswani, N. Shazeer, N. Parmar, J. Uszkoreit, L. Jones, A. N. Gomez, L. u. Kaiser, and I. Polosukhin, "Attention is all you need," in *Proc. NeurIPS*, vol. 30. Curran Associates, Inc., 2017.
- [67] J. Devlin, M. Chang, K. Lee, and K. Toutanova, "BERT: pre-training of deep bidirectional transformers for language understanding," in *Proc. NAACL*, 2019, pp. 4171–4186.
- [68] J. Deng, J. Guo, N. Xue, and S. Zafeiriou, "Arcface: Additive angular margin loss for deep face recognition," in *Proc. CVPR*, 2019.
- [69] J. S. Chung, A. Nagrani, and A. Zisserman, "Voxceleb2: Deep speaker recognition," in *Proc. INTERSPEECH*, 2018, pp. 1086–1090.
- [70] Y. Lin, M. Cheng, F. Zhang, Y. Gao, S. Zhang, and M. Li, "Voxblink2: A 100k+ speaker recognition corpus and the open-set speaker-identification benchmark," in *Proc. INTERSPEECH*, 2024, pp. 4263–4267.
- [71] Z. Gao, Z. Li, J. Wang, H. Luo, X. Shi, M. Chen, Y. Li, L. Zuo, Z. Du, and S. Zhang, "Funasr: A fundamental end-to-end speech recognition toolkit," in *Proc. INTERSPEECH*, 2023, pp. 1593–1597.
- [72] N. Ryant, K. Church, C. Cieri, A. Cristia, J. Du, S. Ganapathy, and M. Liberman, "The second dihard diarization challenge: Dataset, task, and baselines," in *Proc. INTERSPEECH*, 2019, pp. 978–982.
- [73] N. Ryant, P. Singh, V. Krishnamohan, R. Varma, K. Church, C. Cieri, J. Du, S. Ganapathy, and M. Liberman, "The third dihard diarization challenge," in *Proc. INTERSPEECH*, 2021, pp. 3570–3574.
- [74] A. Nagrani, J. S. Chung, and A. Zisserman, "Voxceleb: A large-scale speaker identification dataset," in *Proc. INTERSPEECH*, 2017, pp. 2616–2620.
- [75] G. Hinton, "Distilling the knowledge in a neural network," *arXiv preprint arXiv:1503.02531*, 2015.
- [76] D. Snyder, G. Chen, and D. Povey, "Musan: A music, speech, and noise corpus," *arXiv preprint arXiv:1510.08484*, 2015.
- [77] T. Ko, V. Peddinti, D. Povey, M. L. Seltzer, and S. Khudanpur, "A study on data augmentation of reverberant speech for robust speech recognition," in *Proc. ICASSP*, 2017, pp. 5220–5224.
- [78] I. Loshchilov, "Decoupled weight decay regularization," *arXiv preprint arXiv:1711.05101*, 2017.
- [79] Y. Yue, J. Du, M.-K. He, Y. Yeung, and R. Wang, "Online speaker diarization with core samples selection," in *Proc. INTERSPEECH*, 2022, pp. 1466–1470.
- [80] Y. Kwon, H.-S. Heo, B.-J. Lee, Y. J. Kim, and J.-W. Jung, "Absolute decision corrupts absolutely: Conservative online speaker diarisation," in *Proc. ICASSP*, 2023, pp. 1–5.
- [81] S. Horiguchi, P. García, Y. Fujita, S. Watanabe, and K. Nagamatsu, "End-to-end speaker diarization as post-processing," in *Proc. ICASSP*, 2021, pp. 7188–7192.
- [82] Z. Chen, B. Han, S. Wang, and Y. Qian, "Attention-based encoder-decoder end-to-end neural diarization with embedding enhancer," *IEEE/ACM Transactions on Audio, Speech, and Language Processing*, vol. 32, pp. 1636–1649, 2024.
- [83] A. Plaquet and H. Bredin, "Powerset multi-class cross entropy loss for neural speaker diarization," in *Proc. INTERSPEECH*, 2023, pp. 3222–3226.
- [84] M.-K. He, J. Du, Q.-F. Liu, and C.-H. Lee, "Ansd-ma-mse: Adaptive neural speaker diarization using memory-aware multi-speaker embedding," *IEEE/ACM Transactions on Audio, Speech, and Language Processing*, vol. 31, pp. 1561–1573, 2023.
- [85] M. Härkönen, S. J. Broughton, and L. Samarakoon, "Eend-m2f: Masked-attention mask transformers for speaker diarization," in *Proc. INTERSPEECH*, 2024, pp. 37–41.
- [86] S. Horiguchi, N. Yalta, P. Garcia, Y. Takashima, Y. Xue, D. Raj, Z. Huang, Y. Fujita, S. Watanabe, and S. Khudanpur, "The hitachi-jhu dihard iii system: Competitive end-to-end neural diarization and x-vector clustering systems combined by dover-lap," *arXiv preprint arXiv:2102.01363*, 2021.